Quantum jumps of saturation level rigidity and anomalous oscillations of level number variance in the semiclassical spectrum of a modified Kepler problem

J. M. A. S. P. Wickramasinghe, B. Goodman, and R. A. Serota
Department of Physics, University of Cincinnati, Cincinnati, Ohio 45221-0011, USA
(Received 19 April 2007; revised manuscript received 14 January 2008; published 29 May 2008)

We observe numerically, and explain analytically, a previously unknown phenomenon of quantum-Hall-like jumps in saturation spectral rigidity in the semiclassical spectrum of a modified Kepler problem as a function of the interval center. These jumps correspond to integer decreases of the radial winding numbers in classical periodic motion. We also observe and explain single-harmonic-dominated oscillations of the level number variance with the width of the energy interval. The level number variance becomes effectively zero for the interval widths defined by the frequency of the shortest periodic orbit. This signifies that there are *virtually no variations from sample to sample* in the number of levels on such intervals.

DOI: 10.1103/PhysRevE.77.056216 PACS number(s): 82.40.Bj, 05.30.−d, 05.90.+m, 02.50.−r

I. INTRODUCTION

Level correlations in the semiclassical spectra of classically integrable systems have recently received renewed attention. The most important development was the realization of the long-range nature of such correlations [1], which was explored for rectangular billiards. While it had been previously known that the short-range correlations are absent, the fact reflected by the Poisson statistics of the nearest-neighbor level spacings [2], the evidence for the long-range correlations was indirect—namely, through the saturation property of the spectral rigidity [3,4]. In [1] the correlation function of the level density was obtained, which explicitly describes the long-range correlations in the energy spectrum. Furthermore, in terms of an easily measured quantity, the variance of the number of levels on an energy interval was investigated and was shown to have very unusual properties. Namely, for an interval width narrower than the energy scale associated with the inverse time of the shortest periodic orbit (traversal along the smaller side of the rectangle), the variance equals, in the lowest approximation, the mean number of levels in the interval, indicating the absence of correlations in level positions. For intervals wider than such an energy scale, the variance exhibits nondecaying oscillations around a mean "saturation value" with the amplitude smaller, yet parametrically comparable to the mean value and with the "period" of the same order as the above-mentioned scale (the width of the interval at which the transition from the uncorrelated with correlated behavior occurs).

While such behavior of the variance had been previously predicted via a formal mathematical approach [5], Ref. [1] established that it is a direct consequence of the long-range correlations between energy levels. Two independent analytical derivations were produced [1]: one based on the direct use of quantum mechanical expressions for the energy levels for a particle in a box [6] and the other based on semiclassical periodic orbit theory [3]. Within the latter, it was shown that the oscillations of the variance can be explained by just a few shortest periodic orbits. These results were confirmed numerically with the use of an ensemble-averaging procedure wherein rectangles of the same area, but varying aspect ratios, were used. The reason why the oscillations of the variance can be considered counterintuitive is because with an increase of the interval width and corresponding increase of the mean number of levels, the fluctuation of the number of levels in the interval may actually decrease.

It should be pointed out that the only reason that the variance does not become zero for a rectangular box is that the harmonics that correspond to the shortest periodic orbits have incommensurate frequencies and thus add incoherently [1]. If one could find an integrable system where the variance is dominated by a single periodic orbit harmonic, it could be near zero for certain widths of the energy interval. This would be even more counterintuitive as statistically independent systems would produce different local level structures, yet their total number of levels for such intervals would be nearly the same. In this work we report finding just such a system—the modified Coulomb problem—and, in addition to examining the variance, we find also that the saturation value of the spectral rigidity [7] exhibits quantum jumps associated with the change in the winding number ratio of radial and angular motions of periodic orbits.

In Sec. II, we first review the semiclassical theory of level correlations: its basic equations and features, plus some results in Ref. [1]. In Sec. III, we give an analytical description of the modified Coulomb problem and derive expressions for the saturation spectral rigidity and for the level number variance. We then present the numerical calculations of these quantities, the key results of which are an almost single-harmonic oscillation of the variance and the "quantum-Hall-effect"-like jumps in saturation rigidity.

II. PERIODIC ORBIT THEORY OF LEVEL CORRELATIONS

Following Ref. [1], we consider the intervals $[\varepsilon - E/2, \varepsilon + E/2]$, $E \ll \varepsilon$, where the states with energies near ε have large quantum numbers and can be described semiclassically. Denote by $\mathcal{N}(\varepsilon)$ the cumulative number of levels (or spectral staircase) [2]

$$\mathcal{N}(\varepsilon) = \sum_k \theta(\varepsilon - \varepsilon_k), \tag{1}$$

where θ is unit step function and k labels the energy eigenstates. A "universal" representation of the staircase data is obtained by rescaling the energy variable:

$$\varepsilon \to \varepsilon'(\varepsilon) \equiv \langle \mathcal{N}(\varepsilon) \rangle. \tag{2}$$

Here $\langle \cdots \rangle$ denotes the ensemble average used. In particular, to a computed eigenvalue ε_k the value $\varepsilon'_k = \langle \mathcal{N}(\varepsilon_k) \rangle$ is assigned, so

$$\langle \mathcal{N}'(\varepsilon') \rangle = \langle \mathcal{N}(\varepsilon) \rangle = \varepsilon' \tag{3}$$

and the mean level density is *unity* in the scaled variable:

$$\langle \rho'(\varepsilon') \rangle = \left\langle \sum_k \delta(\varepsilon' - \varepsilon'_k) \right\rangle = 1, \tag{4}$$

$$\Delta = \langle \rho \rangle^{-1} = 1. \tag{5}$$

In practice, we need an approximate analytic form of $\langle \mathcal{N}(\varepsilon) \rangle$ to define the scaled energy-axis variable. Then the staircase representation of the numerical data has a near-45° average slope.

The present work concentrates on long-range correlations in the eigenvalue spectrum—but we remark in passing that the nearest-neighbor level spacings follow the Poisson statistics expected for a classically integrable system [2].

As in Ref. [1], the following two "standard" measures [3,7] for the statistics of large numbers of levels is used here. First, the spectral rigidity $\Delta_3(\varepsilon;E)$—namely, the error of the least-squares fit to linear behavior of the spectral staircase in the interval $[\varepsilon - E/2, \varepsilon + E/2]$,

$$\Delta_3(\varepsilon;E) = \left\langle \min_{(A,B)} \frac{1}{E} \int_{\varepsilon - E/2}^{\varepsilon + E/2} d\varepsilon [\mathcal{N}(\varepsilon) - A - B\varepsilon]^2 \right\rangle, \tag{6}$$

whose explicit form is given by

$$\left\langle \frac{1}{E} \int_{\varepsilon - E/2}^{\varepsilon + E/2} d\varepsilon \mathcal{N}^2(\varepsilon) - \frac{1}{E^2} \left[\int_{\varepsilon - E/2}^{\varepsilon + E/2} d\varepsilon\, \mathcal{N}(\varepsilon) \right]^2 - \frac{12}{E^4} \left[\int_{\varepsilon - E/2}^{\varepsilon + E/2} d\varepsilon\, \varepsilon \mathcal{N}(\varepsilon) \right]^2 \right\rangle, \tag{7}$$

and second, the variance

$$\Sigma(\varepsilon;E) = \langle (N - \langle N \rangle)^2 \rangle \tag{8}$$

of the number of levels N on the interval $[\varepsilon - E/2, \varepsilon + E/2]$:

$$N(\varepsilon;E) = \mathcal{N}\left(\varepsilon + \frac{E}{2}\right) - \mathcal{N}\left(\varepsilon - \frac{E}{2}\right). \tag{9}$$

In the representation (2)–(5), $\langle N \rangle = E$.

The fluctuation measures Σ and Δ_3 can be expressed in terms of the correlation function of the density of levels [7],

$$K(\varepsilon_1, \varepsilon_2) = \langle \delta\rho(\varepsilon_1) \delta\rho(\varepsilon_2) \rangle, \tag{10}$$

$$\delta\rho(\varepsilon) = \rho(\varepsilon) - \langle \rho(\varepsilon) \rangle, \tag{11}$$

regardless of the form of $K(\varepsilon_1, \varepsilon_2)$—for instance,

$$\Sigma(\varepsilon;E) = \int_{\varepsilon - E/2}^{\varepsilon + E/2} \int_{\varepsilon - E/2}^{\varepsilon + E/2} K(\varepsilon_1, \varepsilon_2) d\varepsilon_1 d\varepsilon_2. \tag{12}$$

Using these relationships one can further show that Σ supersedes Δ_3 via an integral relationship [7]

$$\Delta_3(\varepsilon;E) = \frac{2}{E^4} \int_0^E dx (E^3 - 2xE^2 + x^3) \Sigma(\varepsilon, x). \tag{13}$$

In the periodic orbit theory, the correlation function (10) can be expressed as a sum over classical periodic orbits [3]. The important energy scale in the system is that associated with the period of the shortest periodic orbit:

$$E_{\max} \sim \hbar / T_{\min}.$$

For instance, in classically chaotic systems $E_{\max} \sim \Delta$ and for classically integrable systems $E_{\max} \sim \sqrt{\varepsilon \Delta}$ [1]. For energies $E \ll E_{\max}$, the levels are uncorrelated and one finds

$$K(\varepsilon_1, \varepsilon_2) \simeq \delta(\varepsilon_2 - \varepsilon_1), \tag{14}$$

$$\Delta_3(\varepsilon;E) \simeq E/15, \tag{15}$$

$$\Sigma(\varepsilon;E) \simeq E. \tag{16}$$

In the opposite limit $E \gg E_{\max}$, the properties of spectral correlations are very different for the classically chaotic and classically integrable systems [1]. For the former, they are well known and are described by random matrix theory [7] and the supersymmetric nonlinear σ model [8]. For the latter, it was believed that they lead to the saturation rigidity given by [3]

$$\Delta_3^{\infty}(\varepsilon;E) = \frac{2}{\hbar^{N-1}} \sum_j \frac{A_j^2}{T_j^2}, \tag{17}$$

where A_j and T_j are the amplitudes and the periods of the periodic orbits and $2N$ is the dimension of phase space.

It turns out, however, that the more precise formulas, up to the leading terms $E_{\max}/E$, are as follows [1,3]:

$$K^{\infty}(\varepsilon_1, \varepsilon_2) \simeq \frac{2}{\hbar^{N+1}} \sum_j A_j^2 \cos\left(\frac{(\varepsilon_1 - \varepsilon_2) T_j}{\hbar} \right), \tag{18}$$

$$\Delta_3^{\infty}(\varepsilon;E) \simeq \bar{\Delta}_3^{\infty}(\varepsilon;E) \left[1 - \frac{8}{\hbar^{N-1} \bar{\Delta}_3^{\infty}} \sum_j \frac{A_j^2}{E^2 T_j^4} \cos\left(\frac{E T_j}{\hbar} \right) \right], \tag{19}$$

$$\Sigma^{\infty}(\varepsilon;E) \simeq \sum_j \frac{8 A_j^2}{\hbar^{N-1} T_j^2} \sin^2\left(\frac{E T_j}{2\hbar} \right) = \bar{\Sigma}^{\infty}(\varepsilon;E) \left[1 - \frac{4}{\hbar^{N-1} \bar{\Sigma}^{\infty}} \sum_j \frac{A_j^2}{T_j^2} \cos\left(\frac{E T_j}{\hbar} \right) \right], \tag{20}$$

where

$$\bar{\Delta}_3^{\infty}(\varepsilon;E) = \frac{2}{\hbar^{N-1}} \sum_j \frac{A_j^2}{T_j^2}, \quad \bar{\Sigma}^{\infty}(\varepsilon;E) = 2 \bar{\Delta}_3^{\infty}. \tag{21}$$

In the above equations, the superscript "∞" refers to "saturation behavior" and the overbar to averaging over the oscillations. Note that both A_j and T_j depend explicitly on the position of the center of the interval $\varepsilon \gg E$. For instance, in a

rectangular, with the aspect ratio of its sides $L_2/L_1=\alpha_{asp}^{1/2}$, one finds [3] that the periods are integers (representing the number of retracings) of irreducible cycles $\mathbf{M}=\{M_1,M_2\}$,

$$T_{\mathbf{M}}=2\hbar\sqrt{\frac{\pi}{\varepsilon\Delta}(M_1^2\alpha_{asp}^{1/2}+M_2^2\alpha_{asp}^{-1/2})}, \tag{22}$$

where M_1 and M_2 are coprime "winding numbers" of classical periodic orbits such that

$$M_1T_1=M_2T_2, \tag{23}$$

$T_{1,2}$ being the periods of motion along the sides $L_{1,2}$. Expressions for A_j^2 and resulting formulas for the quantities of interest can be found in Refs. [3] and [1].

The key consequences of the above results are as follows. First, the amplitude of oscillations around $\bar{\Delta}_3^{\infty}(\varepsilon;E)$ decays with the width of the interval E. Conversely, the amplitude of oscillations around $\bar{\Sigma}^{\infty}(\varepsilon;E)$ does not decay with an increase of E; furthermore, this amplitude is of the order of $\bar{\Sigma}^{\infty}(\varepsilon;E)$. Second, the amplitudes of oscillations decrease rapidly with the period of periodic orbits. In a rectangle, for instance, $A_j^2\propto T_j^{-1}$ and, using Eq. (22), it is easy to see that just a few terms with smallest winding numbers should dominate the sums in the above equations; this was indeed confirmed numerically [1].

To further appreciate these consequences, consider the contribution from a single harmonic only and compare the result with the known behavior of $\Sigma^{\infty}(\varepsilon;E)$ in a completely uncorrelated system, in an almost rigid spectrum (Gaussian ensemble) and completely rigid spectrum (harmonic oscillator). It is convenient to consider the derivative $\partial\Sigma^{\infty}(\varepsilon;E)/\partial E$, for which we find [1,7]

	Uncorrelated (integrable short range)	Nearly rigid (Gaussian ensembles)	Rigid (harmonic oscillator)	Oscillatory (integrable long range)
$\frac{\partial\Sigma^{\infty}(\varepsilon;E)}{\partial E}\propto$	1	E^{-1}	0	$\frac{4E}{\hbar^{N-2}}\sum_{j:\text{short}}\frac{A_j^2}{T_j}\sin\left(\frac{ET_j}{\hbar}\right)$

where the summation is limited to the few shortest periodic orbits and their corresponding harmonics. Clearly, depending on the interval width E, the oscillatory behavior above of $\partial\Sigma^{\infty}(\varepsilon;E)/\partial E$ spans values from uncorrelated (1) to rigidly distributed (0) spectrum and can even be *negative*, implying a seemingly paradoxical result where the fluctuation of the number of levels decreases as the average interval width (and the mean number of levels) increases.

Finally, because the frequencies of harmonics are incommensurate, $\Sigma^{\infty}(\varepsilon;E)$ ordinarily does not reach zero; it oscillates between $\Sigma_{\max}^{\infty}(\varepsilon;E)$ and $\Sigma_{\min}^{\infty}(\varepsilon;E)$, each typically of order of $\bar{\Sigma}^{\infty}(\varepsilon;E)$ parametrically (for a particle in the box, see [1]). However, if one can find a system where the shortest periodic orbit T_0 dominates the sum, $\Sigma^{\infty}(\varepsilon;E)$ can be reduced, as per Eqs. (20) and (21), to

$$\Sigma^{\infty}(\varepsilon;E)\simeq 2\bar{\Sigma}^{\infty}(\varepsilon;E)\sin^2\left(\frac{ET_0}{2\hbar}\right)$$

and can become effectively zero for $E=2\hbar n\pi T_0^{-1}$. The same effect would be also achieved if the periods of other periodic orbits are integer multiples of T_0. We found such a system in a modified Coulomb problem, which we proceed to discuss below.

III. MODIFIED COULOMB MODEL

We consider a particle in the central potential

$$V(r)=-\frac{\alpha}{r}+\frac{\beta}{r^2}. \tag{24}$$

Classically, the trajectory of the motion is given by [9]

$$r=\frac{p}{1+e\cos\gamma(\theta-\theta_0)}, \tag{25}$$

where

$$p=\frac{2}{\alpha}\left(\beta+\frac{L^2}{2m}\right), \tag{26}$$

$$e=\sqrt{1+\frac{4\varepsilon}{\alpha^2}\left(\beta+\frac{L^2}{2m}\right)}, \tag{27}$$

$$\gamma=\sqrt{1+\frac{2m\beta}{L^2}}. \tag{28}$$

Using the canonical action variables [10]

$$I_r=-\sqrt{L^2+2m\beta}+\alpha\sqrt{\frac{m}{2|\varepsilon|}},\quad I_\theta=L, \tag{29}$$

we can express the energy as

$$\varepsilon=-\frac{m\alpha^2}{2(I_r+\sqrt{I_\theta^2+2m\beta})^2} \tag{30}$$

and rewrite the expressions for p and e as

$$p = \frac{I_\theta^2}{m\alpha} \quad \text{and} \quad e^2 = 1 - \left(\frac{I_\theta}{I_r + I_\theta}\right)^2, \tag{31}$$

respectively.

The frequencies of radial and angular motion are given by [9]

$$\omega_r = \frac{\partial \varepsilon}{\partial I_r} = \sqrt{\frac{(2|\varepsilon|)^3}{m\alpha^2}} = 2\sqrt{\frac{|\varepsilon|^3}{2m\beta\bar{\varepsilon}}}, \tag{32}$$

$$\omega_\theta = \frac{\partial \varepsilon}{\partial I_\theta} = \frac{\omega_r}{\gamma}, \tag{33}$$

where the notation

$$\bar{\varepsilon} = \frac{\alpha^2}{4\beta} \tag{34}$$

was introduced. For any energy ε, the motion is conditionally periodic except for the following two circumstances.

First, for the values of the angular momentum L such that

$$\gamma = \frac{M_r}{M_\theta} - \text{rational}, \tag{35}$$

the motion becomes periodic with the periods of radial and angular motions related by

$$T_\theta = \gamma T_r \quad \text{or} \quad M_\theta T_\theta = M_r T_r \equiv T_{\mathbf{M}}. \tag{36}$$

Here $T_{\mathbf{M}}$ is the period of an irreducible cycle $\mathbf{M}=\{M_r, M_\theta\}$ (M_r and M_θ are coprime), whose orbital and angular winding numbers are, respectively, M_r and M_θ. In other words, the orbit closes for the first time after M_r periods of radial motion and M_θ periods of angular motion.

Second, from

$$e = 0 \Leftrightarrow I_r = 0, \tag{37}$$

the motion becomes circular for L such that

$$L^{(cir)} = \sqrt{2m\beta}\sqrt{\frac{\bar{\varepsilon} - |\varepsilon|}{|\varepsilon|}}, \tag{38}$$

in which case $\mathbf{M}=\{0,1\}$. From Eqs. (28) and (29) the corresponding frequency is found as

$$\omega_\theta^{(cir)} = \frac{\omega_r}{\gamma^{(cir)}}, \tag{39}$$

$$\gamma^{(cir)} = \sqrt{\frac{\bar{\varepsilon}}{\bar{\varepsilon} - |\varepsilon|}}, \tag{40}$$

where ω_r is still given by (32) but, since the distance from the center remains fixed, does not have the meaning of a radial frequency.

It is very important to notice that ω_r depends only on the energy ε and does not depend on the angular momentum L. As was already mentioned, at any energy ε the conditionally periodic motion becomes periodic for such values of L that γ is rational; these values, however, do not depend on ε, except for the constraint

$$\gamma = \left(\sqrt{\frac{\bar{\varepsilon}}{|\varepsilon|}} - \frac{I_r}{\sqrt{2m\beta}}\right) \Bigg/ \sqrt{\left(\sqrt{\frac{\bar{\varepsilon}}{|\varepsilon|}} - \frac{I_r}{\sqrt{2m\beta}}\right)^2 - 1} \geq \gamma^{(cir)}, \tag{41}$$

which follows from Eqs. (28) and (40). Consequently, the following picture of the periodic orbits emerges. In addition to circular orbits, whose period

$$T^{(cir)} = \frac{2\pi}{\omega_r}\gamma^{(cir)} \tag{42}$$

is given by Eqs. (32) and (40) and changes continuously as a function of energy, there are irreducible orbits such that

$$M_r = [M_\theta \gamma^{(cir)}] + i, \tag{43}$$

where $[\cdots]$ is the floor function and i are integers such that M_r and M_θ are coprime. These correspond to rational γ's, Eq. (35), and their period is given by

$$T_{\mathbf{M}} = \frac{2\pi}{\omega_r} M_r = T_r M_r. \tag{44}$$

In view of inequality (41), new rational values of γ become possible at discrete (quantized) values of ε. In particular, the shortest periodic orbits

$$M_\theta = 1, \quad \gamma = M_r = M_r^{\min} + i, \tag{45}$$

$$M_r^{\min} = [\gamma^{(cir)}] + 1, \quad i < \gamma^{(cir)}, \tag{46}$$

are especially important. The key observation here is that as ε increases ($|\varepsilon|$ decreases), the smaller values of M_r become possible, with quantum jumps occurring for energies such that $\gamma^{(cir)}$ is integer. This fact will prove to be crucial in evaluation of the spectral rigidity and level number variance. Finally, for either type of periodic orbit, it can be subsequently retraced with the period of $nT_{\mathbf{M}}$, where n is the number of retracings.

IV. SEMICLASSICAL SPECTRUM

The quantum spectrum is given by [11]

$$\varepsilon_{p,l} = -\frac{2m\alpha^2}{\hbar^2[2p + 1 + \sqrt{(2l+1)^2 + 2m\beta/\hbar^2}]^2} \simeq -\frac{m\alpha^2}{2\hbar^2(p + \sqrt{l^2 + 2m\beta/\hbar^2})^2}, \tag{47}$$

which clearly follows from (30) via Born-Sommerfeld. quantization of the action variables

$$I_r = \hbar\left(p + \frac{1}{2}\right), \quad I_\theta = \hbar\left(l + \frac{1}{2}\right), \tag{48}$$

and the second of Eqs. (47) is the limit of large quantum numbers, $p, l \gg 1$, that in the semiclassical approximation used here. Further, we make yet another approximation that is concerned with the fact that the standard Kepler problem (Bohr atom in the quantum limit) is a so called "supersymmetric" or "resonant" problem [2]. This is because the fre-

quency of radial and angular motions coincide in the Kepler problem (so that the motion is periodic), which is indicative of extra symmetry in the problem, as well as additional conserved quantities—Runge-Lenz vector in the present case. In the Bohr atom, the latter is associated with the n^2-fold degeneracy of the n's energy eigenstate. Conversely, in a "generic" (nonresonant) integrable system, the motion is ordinarily conditionally periodic, except for specific values of certain parameters upon which the motion may become periodic. Thus, in order to achieve the greatest possible difference with the standard Kepler problem, a large parameter β must be considered in (24). Accordingly, we assume that the condition $\beta/a_B^2 \gg \alpha/a_B$ holds, where $a_B=\hbar^2/m\alpha$ is the Bohr radius—that is, $m\beta/\hbar^2 \gg 1$. This condition translates, as follows from (47), to that of the quantum numbers p and l being limited from above, which, combined with the semiclassical approximation, yields

$$1 \ll p,l \ll \sqrt{\frac{2m\beta}{\hbar^2}}, \quad \frac{m\beta}{\hbar^2} \gg 1. \tag{49}$$

Using (49) to expand Eq. (47), we obtain

$$\varepsilon_{p,l} \approx -\frac{\alpha^2}{4\beta} + \frac{\alpha^2}{4\beta}\frac{2p\sqrt{2m\beta/\hbar^2}+l^2}{2m\beta/\hbar^2} \equiv -\bar{\varepsilon} + \bar{\varepsilon}\frac{\epsilon_{p,l}}{2\beta}, \tag{50}$$

and with a substitution

$$\frac{m\beta}{\hbar^2} \to \beta, \tag{51}$$

we find

$$\epsilon_{p,l} = 2p\sqrt{2\beta} + l^2 \ll 2\beta. \tag{52}$$

Classically, the condition corresponding to (49) would be

$$I_\theta \ (=L), \quad I_r \ll \sqrt{2m\beta}, \tag{53}$$

leading to

$$\varepsilon \approx -\bar{\varepsilon} + \bar{\varepsilon}\frac{2I_r\sqrt{2m\beta}+I_\theta^2}{2m\beta} \equiv -\bar{\varepsilon} + \bar{\varepsilon}\frac{\epsilon}{2\beta}, \tag{54}$$

where

$$\epsilon = 2I_r\sqrt{2\beta} + I_\theta^2 \ll 2\beta \tag{55}$$

and $I_{r,\theta} \to I_{r,\theta}/\hbar$ are now dimensionless.

Obviously, in both quantum and classical circumstances, $\varepsilon \approx -\bar{\varepsilon}$ in the zeroth order. The latter leads to simplified formulas for the frequencies since in this approximation

$$\omega_r \approx \frac{2\bar{\varepsilon}}{\sqrt{2m\beta}}, \quad \omega_\theta = \frac{\omega_r}{\gamma}, \tag{56}$$

and, from Eqs. (40) and (54),

$$\gamma \geq \gamma^{(cir)} = \sqrt{\frac{2\beta}{\epsilon}} \gg 1, \tag{57}$$

as follows from (55).

Due to the linear relationship between ε and ϵ in (50), the spectral properties of the two are identical. Consequently, in what follows, it is the spectrum (52) that is studied numerically. Similarly to the rectangle, where ensemble averaging was understood in terms of variations of the rectangle's aspect ratio [1], here ensemble averaging is understood in terms of the variations of β. Flattening of the spectrum is achieved via (2) with

$$\langle \mathcal{N}(\epsilon) \rangle \approx \frac{\epsilon^{3/2}}{3\sqrt{2\beta}}, \tag{58}$$

which follows immediately from Eqs. (1) and (52). This is equivalent to starting with the scaled Hamiltonian

$$\epsilon_{sc} = \frac{(2I_r\sqrt{2\beta}+I_\theta^2)^{3/2}}{3\sqrt{2\beta}}, \tag{59}$$

for which

$$\langle \mathcal{N}(\epsilon_{sc}) \rangle = \epsilon_{sc}.$$

In what follows, we will drop subscript "*sc*." The frequencies are now given by

$$\omega_r = (\sqrt{2\beta}3\epsilon)^{1/3}, \quad \omega_\theta = \frac{\omega_r}{\gamma}, \tag{60}$$

where

$$\gamma = \sqrt{\frac{2\beta}{I_\theta^2}} = \sqrt{\frac{2\beta}{(3\epsilon\sqrt{2\beta})^{2/3} - 2I_r\sqrt{2\beta}}} \geq \gamma^{(cir)} = \left(\frac{2\beta}{3\epsilon}\right)^{1/3} \gg 1, \tag{61}$$

obtained by solving (59) for I_θ^2. (For convenience, we carried over the notation $\gamma^{(cir)}$.)

V. LEVEL CORRELATION FUNCTION, SPECTRAL RIGIDITY, AND LEVEL NUMBER VARIANCE

We now turn to evaluation of the level correlation function (18). Using the result obtained in the Appendix, we find

$$K^\infty(\epsilon_1,\epsilon_2) = \sum_{\mathbf{M}} \frac{\omega_r}{3\epsilon M_r}\cos\left(\frac{2\pi(\varepsilon_1-\varepsilon_2)M_r}{\omega_r}\right). \tag{62}$$

To reduce this to the sum on M_r only, we notice that from (61) and (46),

$$M_r^{\min} = [\gamma^{(cir)}] + 1. \tag{63}$$

Second, for each M_r, there are $[M_r/\gamma^{(cir)}]$ possible values of M_θ, and consequently, we obtain

$$K^\infty(\epsilon_1,\epsilon_2) = \sum_{\mathbf{M}} \frac{\omega_r}{3\epsilon M_r}\left[\frac{M_r}{\gamma^{(cir)}}\right]\cos\left(\frac{2\pi(\varepsilon_1-\varepsilon_2)M_r}{\omega_r}\right). \tag{64}$$

For very small $(\varepsilon_1-\varepsilon_2)$, it is possible to reduce this sum to an integral. Neglecting the difference between the function and its floor, including time-reversal of each orbit, and using Eqs. (60) and (61), we find

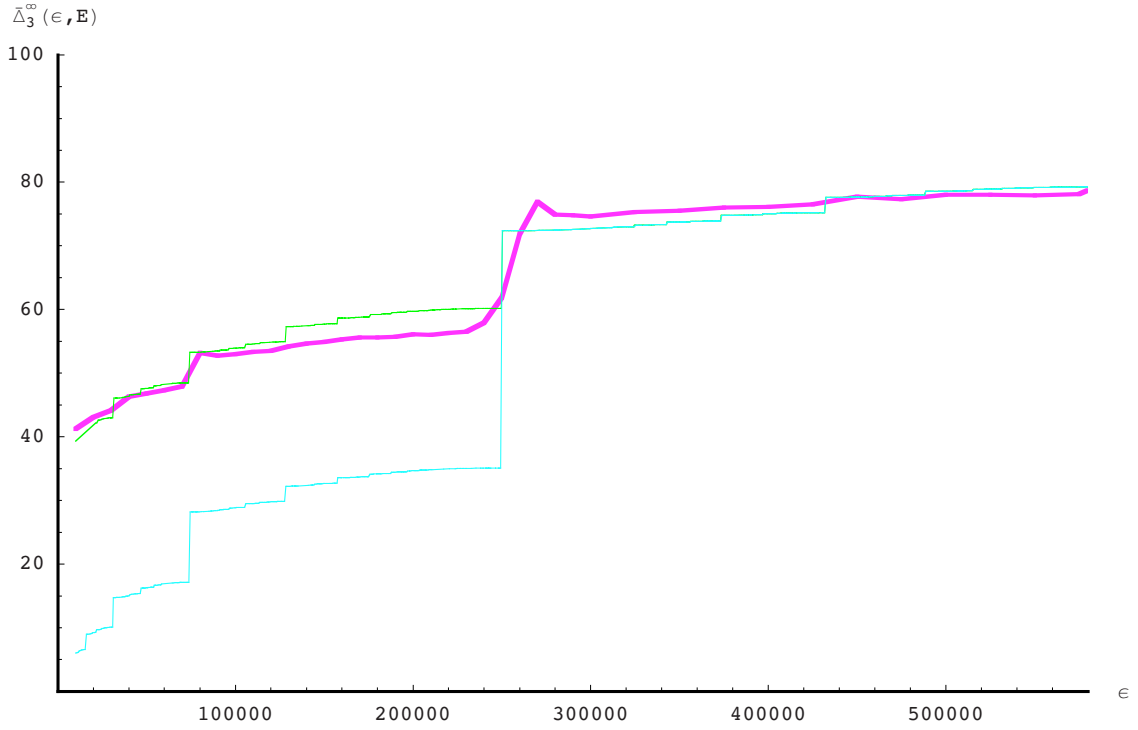

FIG. 1. (Color online) $\bar{\Delta}_3^{\infty}(\epsilon;E)$ vs ϵ for $\beta=3\times10^6$. The thicker line is the numerical simulation while the lower thinner line is the analytical result given by Eq. (69) and the higher one uses the modification (71); the latter two lines coincide on the top plateau since (71) gives zero correction for these values of ϵ.

$$K^{\infty}(\epsilon_1,\epsilon_2) \approx \sum_{M_r=M_r^{\min}} \frac{2\omega_r}{3\epsilon\gamma^{(cir)}}\cos\left(\frac{2\pi(\varepsilon_1-\varepsilon_2)M_r}{\omega_r}\right), \quad (65)$$

$$\approx \frac{1}{\pi}\frac{\omega_r^2}{3\epsilon\gamma^{(cir)}}\int_{T_{\min}} dx\,\cos[(\varepsilon_1-\varepsilon_2)x], \quad (66)$$

$$= \delta(\varepsilon_1-\varepsilon_2) - \frac{\sin[(\varepsilon_1-\varepsilon_2)/\mathcal{E}]}{\pi(\varepsilon_1-\varepsilon_2)}, \quad (67)$$

where

$$\mathcal{E} = T_{\min}^{-1} = \frac{\omega_r}{2\pi M_r^{\min}} \quad (68)$$

and $T_{\min}$ is the period of the shortest periodic orbit. This is in complete analogy to the approximate form of the correlation function found for a rectangular box [1] where the δ-function term corresponds to the absence of level correlations and the second term the onset thereof.

Similarly, the saturation spectral rigidity (21) is given by

$$\bar{\Delta}_3^{\infty}(\epsilon;E) \approx \frac{\sqrt{2\beta}}{\pi^2}\sum_{M_r=M_r^{\min}}\left[\frac{M_r}{\gamma^{(cir)}}\right]\frac{1}{M_r^3} = \frac{\sqrt{2\beta}}{\pi^2}\sum_{M_r=2}\left[\frac{M_r}{\gamma^{(cir)}}\right]\frac{1}{M_r^3}, \quad (69)$$

where E is now understood as the interval width in the spectrum ϵ. The second equality follows from the fact that the floor function in the sum automatically takes care of the summation starting with $M_r^{\min}$.

Together, Eqs. (69), (61), and (63) transparently predict quantum jumps in the saturation level rigidity. As the energy increases, γ_{cir} decreases, and as it takes on smaller integer values, a transition $M_r^{\min}\to M_r^{\min}-1$ takes place, leading to a jump in the saturation rigidity. We observe such jumps in numerical simulations, discussed in the next section.

Finally, the level number variance is given by

$$\Sigma^{\infty}(\epsilon;E) \approx \frac{4\sqrt{2\beta}}{\pi^2}\sum_{M_r=2}\left[\frac{M_r}{\gamma^{(cir)}}\right]\frac{1}{M_r^3}\sin^2\left(\frac{\pi E M_r}{\omega_r}\right), \quad (70)$$

assuring that $\bar{\Sigma}^{\infty}(\epsilon;E)=2\bar{\Delta}_3^{\infty}(\epsilon;E)$.

VI. NUMERICAL SIMULATIONS

We conduct numerical simulations on the spectrum (52) for central values of $\beta=5\times10^5$ and $\beta=1,2,3,4,5\times10^6$. As previously mentioned, "ensemble averaging" is accomplished for each β by taking $\sim$100 values of β around the central value. These β's must be sufficiently close to the central value, so as to eliminate the systematic dependence on β, yet sufficiently far to ensure proper sampling. As a first step, we verified the Poisson (exponential) distribution for the nearest level spacings, which should be the case for an integrable system without extra degeneracies [2,12].

The numerical results for $\bar{\Delta}_3^{\infty}$ in relation to (69) are shown in Fig. 1. While (69) provides a wonderful fit to numerical data on the top plateau, it predicts larger jumps between the

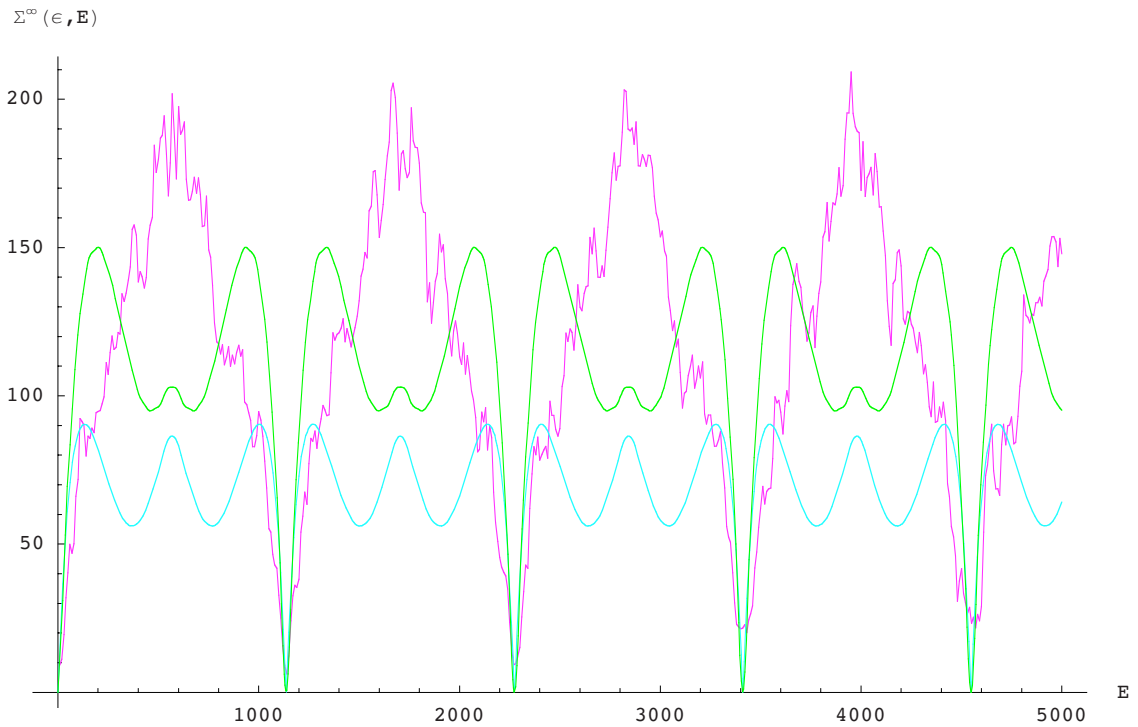

FIG. 2. (Color online) $\Sigma^{\infty}(\epsilon;E)$ vs E for $\beta=3\times10^{6}$ and $\epsilon=2\times10^{5}$. The jagged line is the numerical simulation while the smooth line with smaller amplitude is the analytical result given by Eq. (70) and the one with larger amplitude uses the modification (71).

plateaus than are seen numerically. As a result, to fit lower plateaus we added an empirical constant via the substitution

$$\left[\frac{M_r}{\gamma^{(cir)}}\right] \to \left[\frac{M_r}{\gamma^{(cir)}}\right] + \sum_{n=1}^{[M_r/\gamma^{(cir)}]-1} \frac{1}{2^{2n-1}}. \tag{71}$$

At this time we do not have a good explanation for this discrepancy. Further, the theoretical formula predicts an additional noticeable jump farther up in the spectrum, when $\gamma^{(cir)}=3/2$, which is not seen on the experimental curve. We point out, however, that the above empirical constant does not introduce jumps into the level rigidity, but only adjusts the heights of the lower plateaus. Furthermore, the positions of the observed jumps are in excellent agreement with Eqs. (61) and (63).

With the same modification (71) in Eq. (70), we plot $\Sigma^{\infty}(\epsilon;E)$ as a function of E for two different values of ϵ. Clearly, while the periodicity is superbly predicted by the analytical expression, there is a noticeable difference in the intermediate structure in comparison with the numerical results. One reason for this may be insufficient sampling due to constraints on the number of β's used in the numerical pro-

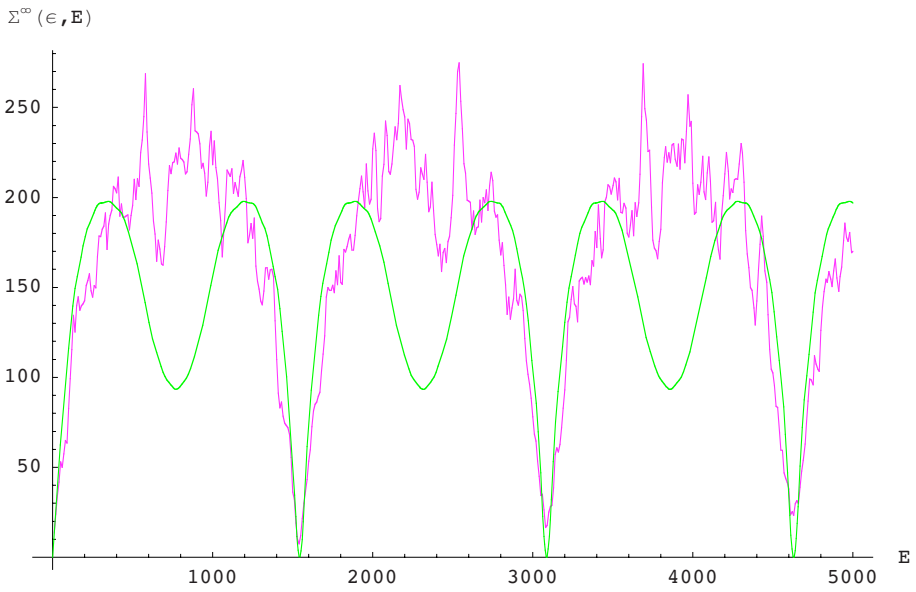

FIG. 3. (Color online) Same as Fig. 2 for $\epsilon=5\times10^{5}$ [for this value of ϵ, there is no correction due to (71)].

cedure (compare Figs. 2 and 3 with corresponding plots in Ref. [1]). Unfortunately, as in the latter case, one cannot improve the statistics much by the usual techniques, such as spectral averaging, as the required widths of the energy windows would lead to sums of incoherent harmonics (beats), leading to the jumps in the level rigidity morphing into a continuous curve, while also eliminating the effect of near-zero values of the level number variance.

VII. CONCLUSIONS

We observe numerically, and explain analytically, quantum-Hall-like jumps of the averaged saturation level rigidity in a modified Coulomb problem. These are explained semiclassically in terms of the jumps in the winding numbers of the shortest periodic orbits as the position of the interval center moves through the energy spectrum. (The analogy with the quantum Hall effect is largely mathematical, as the number of terms in the sum also discontinuously changes by 1, in the latter case, when the top Landau level unloads to the lower levels while moving through the chemical potential with an increase of the magnetic field.) Also, analytically and numerically, we predict sinusoidal oscillations of the saturation level number variance with the interval width. This is a striking result which indicates that, while the distribution of the levels on a interval varies greatly from sample to sample, the total number of levels in the interval may be nearly identical for certain values of the interval width. It comes about because higher harmonics are integer fractions of the shortest periodic orbit and add up coherently. The latter also explains the difference with other systems, such as rectangular boxes, where the oscillations may be large, but the variance does not reach a near-zero value.

In the future, a direct evaluation of the variance, using the formalism of Ref. [6] (similar to a rectangle in Ref. [1]) needs to be done without the use of the periodic orbit theory.

APPENDIX: AMPLITUDES OF PERIODIC ORBITS

The amplitude of an irreducible cycle $\mathbf{M}=\{M_1,M_2\}$ is given by [13]

$$A_{\mathbf{M}}^2 = \frac{2\pi}{T_{\mathbf{M}}^2 |\boldsymbol{\omega}\cdot\partial\mathbf{I}_{\mathbf{M}}/\partial T_{\mathbf{M}}\ \det\{\partial\omega_i/\partial I_k\}_{\mathbf{M}}|}, \tag{A1}$$

$$\boldsymbol{\omega}(\mathbf{I}_{\mathbf{M}})T_{\mathbf{M}} = 2\pi\mathbf{M}. \tag{A2}$$

This equation can be simplified by differentiating (A2) on T, which gives

$$T\sum_{j=1}^{2}\frac{\partial\omega_i}{\partial I_j}\frac{\partial I_j}{\partial T} + \omega_i = 0, \tag{A3}$$

whereof

$$\boldsymbol{\omega}\cdot\partial\mathbf{I}/\partial T = \frac{-[\omega_1^2(\partial\omega_2/\partial I_2)+\omega_2^2(\partial\omega_1/\partial I_1)]+\omega_1\omega_2(\partial\omega_1/\partial I_2+\partial\omega_2/\partial I_1)}{T\ \det\{\partial\omega_i/\partial I_k\}}, \tag{A4}$$

so that[1]

$$A_{\mathbf{M}}^2 = \frac{2\pi}{T_{\mathbf{M}}|-[\omega_1^2(\partial\omega_2/\partial I_2)+\omega_2^2(\partial\omega_1/\partial I_1)]+\omega_1\omega_2(\partial\omega_1/\partial I_2+\partial\omega_2/\partial I_1)|_{\mathbf{M}}}, \tag{A5}$$

which shows a universal dependence of $A_{\mathbf{M}}^2$ on $T_{\mathbf{M}}$.

Here, $\mathbf{I}=\{I_r,I_\theta\}$ and $\boldsymbol{\omega}=\{\omega_r,\omega_\theta\}=\nabla_{\mathbf{I}}\epsilon(\mathbf{I})$, where ϵ is given by (59). Consequently, from (A5), we find

$$A_{\mathbf{M}}^2 = \frac{2\pi}{3\epsilon T_{\mathbf{M}}} = \frac{\omega_r}{3\epsilon M_r},$$

where ω_r is given by (60).

[1]In a more compact form $-[\omega_1^2(\partial\omega_2/\partial I_2)+\omega_2^2(\partial\omega_1/\partial I_1)]+\omega_1\omega_2(\partial\omega_1/\partial I_2+\partial\omega_2/\partial I_1)=[\omega_2\partial(\omega_1/\omega_2)/\partial I_2+\omega_1\partial(\omega_2/\omega_1)/\partial I_1]$. It can also be conveniently rewritten in terms of second derivatives of the energy using the first equations of Eqs. (32) and (33).

[1] J. M. A. S. P. Wickramasinghe, B. Goodman, and R. A. Serota, Phys. Rev. E **72**, 056209 (2005).
[2] Martin C. Gutzwiller, *Classical And Quantum Mechanics* (Springer-Verlag, New York, 1990).
[3] M. V. Berry, Proc. R. Soc. London, Ser. A **400**, 229 (1985).
[4] G. Casati, B. V. Chirikov, and I. Guarneri, Phys. Rev. Lett. **54**, 1350 (1985).
[5] P. M. Bleher and J. L. Lebowitz, J. Stat. Phys. **74**, 167 (1994).
[6] Felix von Oppen, Phys. Rev. B **50**, 17151 (1994).
[7] T. A. Brody, J. Flores, J. B. French, P. A. Mello, A. Pandey, and S. S. M. Wong, Rev. Mod. Phys. **53**, 385 (1981).
[8] Konstantin Efetov, *Disorder And Chaos* (Cambridge University Press, Cambridge, England, 1997).
[9] G. L. Kotkin and V. G. Serbo, *Classical Mechanics* (Pergamon Press, New York, 1971).
[10] L. D. Landau and E. M. Lifshitz, *Mechanics* (Pergamon Press, New York, 1988).
[11] L. D. Landau and E. M. Lifshitz, *Quantum Mechanics* (Pergamon Press, New York, 1981).
[12] M. Robnik and G. Veble, Prog. Theor. Phys. Suppl. **139**, 544 (2000); M. Robnik and G. Veble, J. Phys. A **31**, 4669 (1998).
[13] M. V. Berry and M. Tabor, J. Phys. A **10**, 371 (1977).